

# THE INFLUENCE OF MAGNETIC FIELD ON THE CNM MASS FRACTION AND ITS ALIGNMENT WITH DENSITY STRUCTURES.

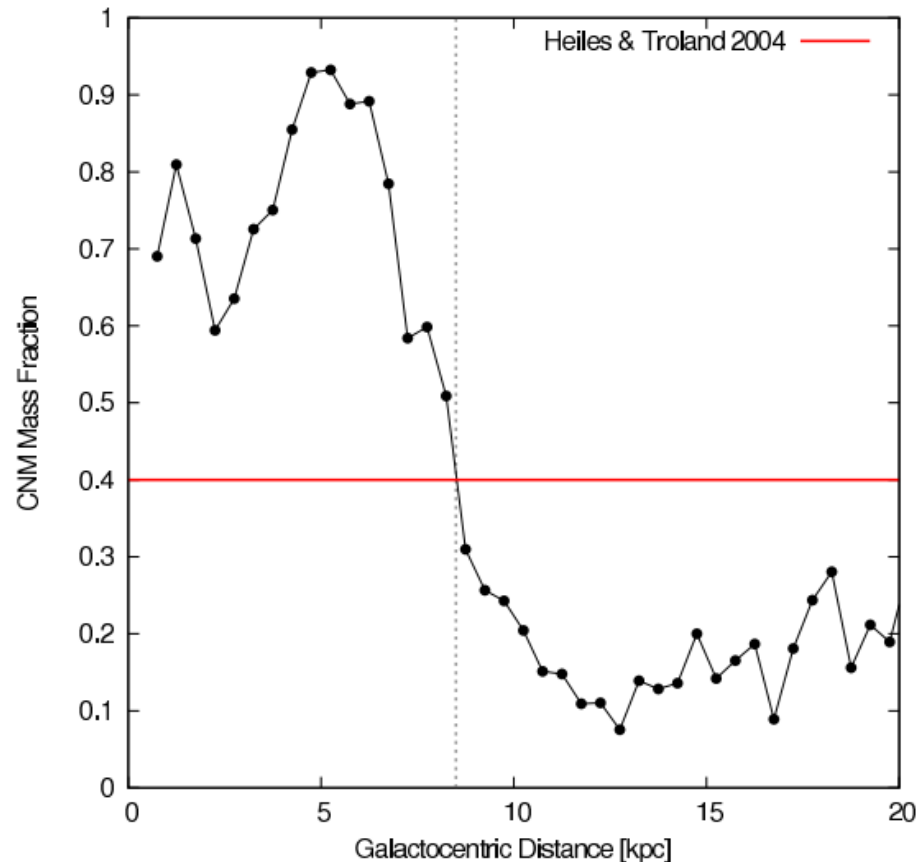
MARCO A. VILLAGRAN\*

Colaborator:  
Adriana Gazol

\*m.villagran@irya.unam.mx



# INTRODUCTION: CNM MASS FRACTION



- The neutral atomic ISM is **multiphasic**. It gets segregated via thermal instability, which is regulated by the physical conditions of the medium. In the solar neighbourhood, an **estimate 40% of the total gas mass is in CNM**, this according to the HI measurements presented in Heiles & Troland (2003) and later confirmed in Pineda et al. (2013), where the authors used the 158  $\mu\text{m}$  CII line observations from Herschel/HIFI, and HI (21 cm),  $^{12}\text{CO}$  and  $^{13}\text{CO}$  maps to separate between the ISM components.

## INTRODUCTION: ALIGNMENT OF CNM WITH **B**

- There is magnetic field associated with the neutral atomic ISM, with a reported value of  $B \sim 6 \mu\text{G}$  given in Beck (2008).
- The local magnetic field seems to be **aligned with the cold diffuse structures** of this medium. This comes from observational works like, Clark et al. (2014) and Planck Collaboration et al. XXXII (2016). The first one using data from the surveys: GALFA-HI and the Parkes Galactic All Sky. The second one, with linearly polarized emission from dust at 353 GHz, obtained with the Planck Satellite.
- We understand the alignment as having a **magnetic field parallel to the gas structures**.

## GOALS & METHODOLOGY

- Our **main goal** is to quantify the effects that **varying the intensity of  $\mathbf{B}$  in MHD simulations** with conditions akin to the solar neighbourhood has on both the CNM mass fraction and the alignment between  $\mathbf{B}$  and the CNM.
- An additional goal is to study the **differences that self-gravity creates** in our models.
- We try to achieve these goals by using MHD simulations, with periodic boundary conditions, Fourier forcing (at a fixed wave number) with a constant energy injection rate and a **cooling function**. The cooling function was previously used in Gazol & Villagran (2016) and it is based on the values given in Wolfire et al. (2003)
- All of our simulations were done in a 512 cells per side (**100 pc**) cube, having a resolution of  **$\sim 0.2$  pc**.

## DATA SET

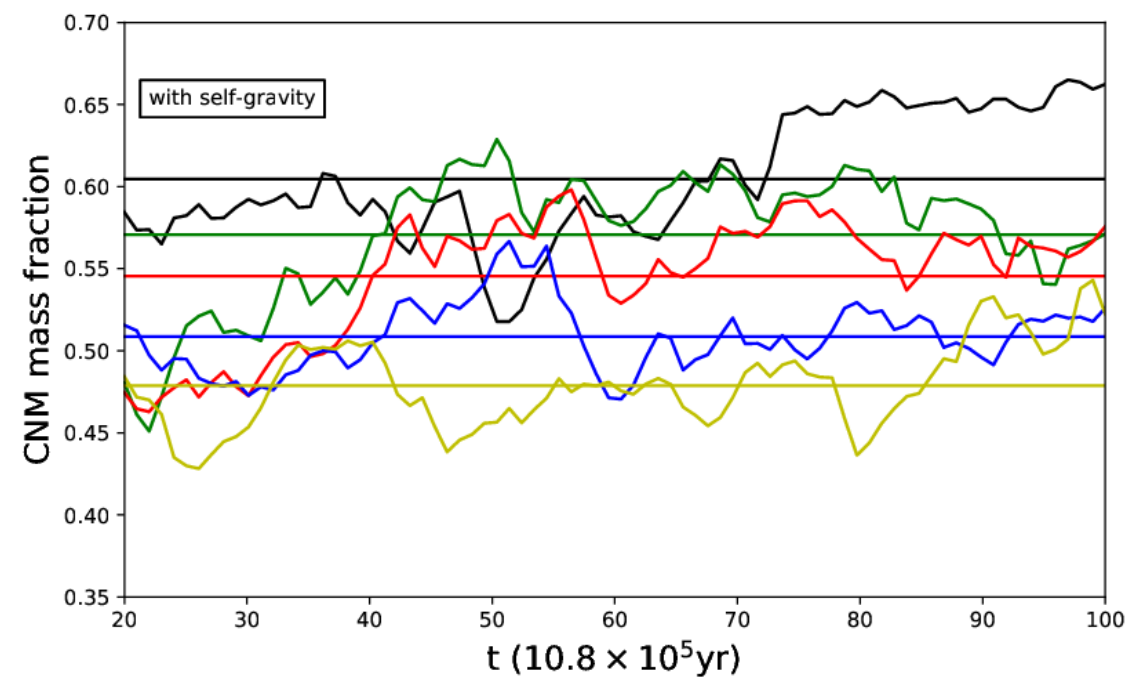
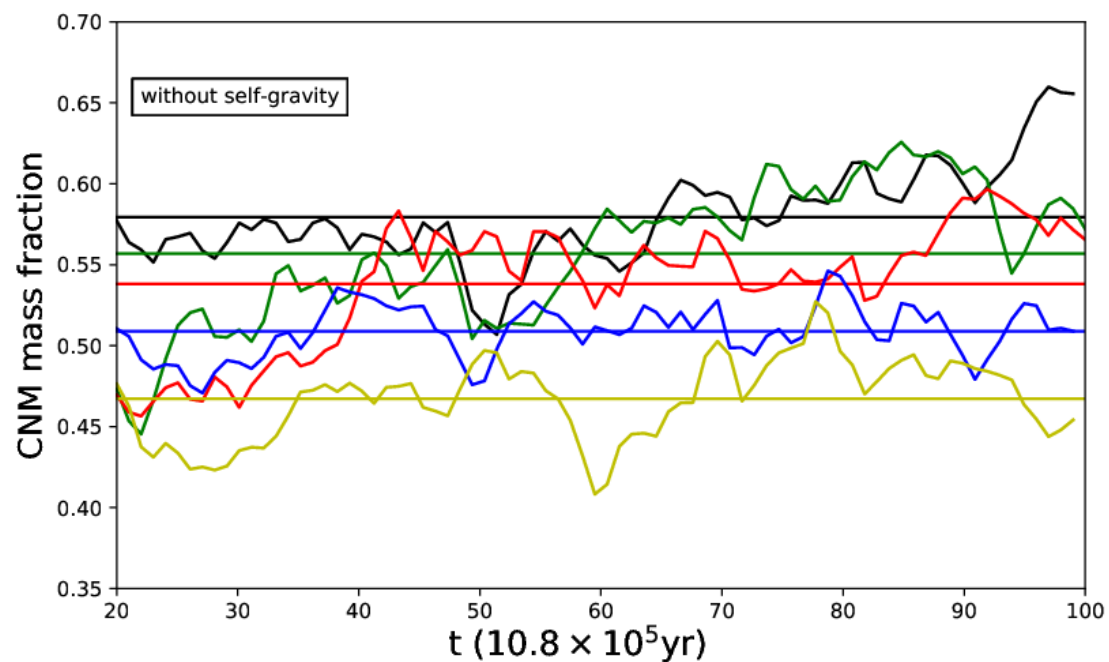
- We have a total of **eighteen simulations**.
- Half of them are self-gravitating.
- We used a base mean density of  $n = 2 \text{ cm}^{-3}$  and two higher ones,  $n = 3 \text{ cm}^{-3}$  and  $n = 4 \text{ cm}^{-3}$ .
- We tested **four initial magnetic fields**,  $B_0 \sim 0.2 \text{ } \mu\text{G}$ ,  $B_0 \sim 2.1 \text{ } \mu\text{G}$ ,  $B_0 \sim 4.2 \text{ } \mu\text{G}$  and  $B_0 \sim 8.3 \text{ } \mu\text{G}$ . Additionally we studied simulations without magnetic field.
- All of our simulations start with a constant magnetic field along the x axis, a uniform thermally unstable density and at rest.

## RESULTS: CNM MASS FRACTIONS

- We calculated the three-dimensional cold gas mass fraction (F3D) and two two-dimensional CNM mass fractions.
- The temperature's upper limit of cold gas is  $T = 278$  K.
- The results are shown in groups of comparable simulations, the most important being the group of all the simulations with mean density  $n = 2 \text{ cm}^{-3}$
- There is little difference between simulations with and without self-gravity.

# RESULTS: 3D CNM MASS FRACTION

Villagran & Gazol (submitted)

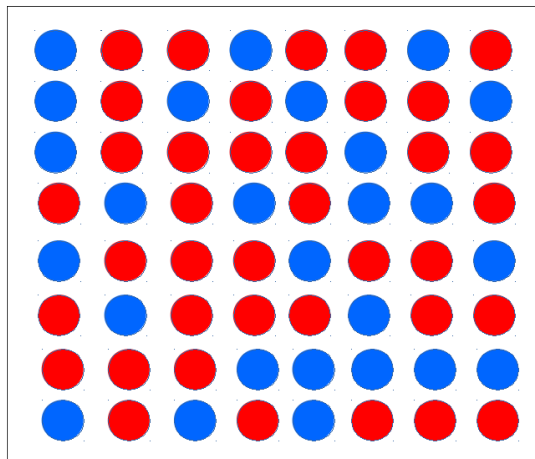


( $n_0 = 2 \text{ cm}^{-3}$ ):  $B_0 = 0.0 \mu\text{G}$ ,  $B_0 \sim 0.4 \mu\text{G}$ ,  $B_0 \sim 2.1 \mu\text{G}$ ,  $B_0 \sim 4.2 \mu\text{G}$ ,  $B_0 \sim 8.3 \mu\text{G}$

**The CNM mass fraction decreases with magnetic field.**

# RESULTS: 2D CNM MASS FRACTION

- The two-dimensional projections are perpendicular (YZ) and parallel (XZ) to the initial magnetic field, i.e. the x axis.
- The two-dimensional fractions were calculated by two different methods. The first one takes into account all the lines of sight in our plane (F2D) and the second one only the lines of sight with cold gas on them (F2D0)



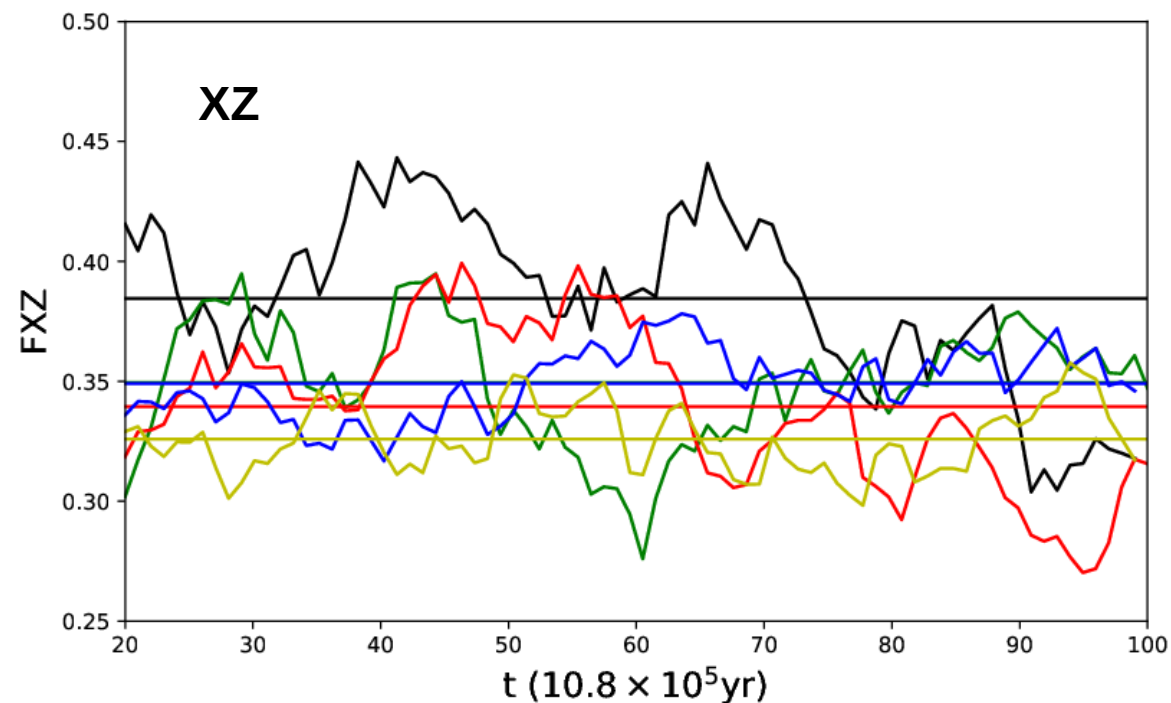
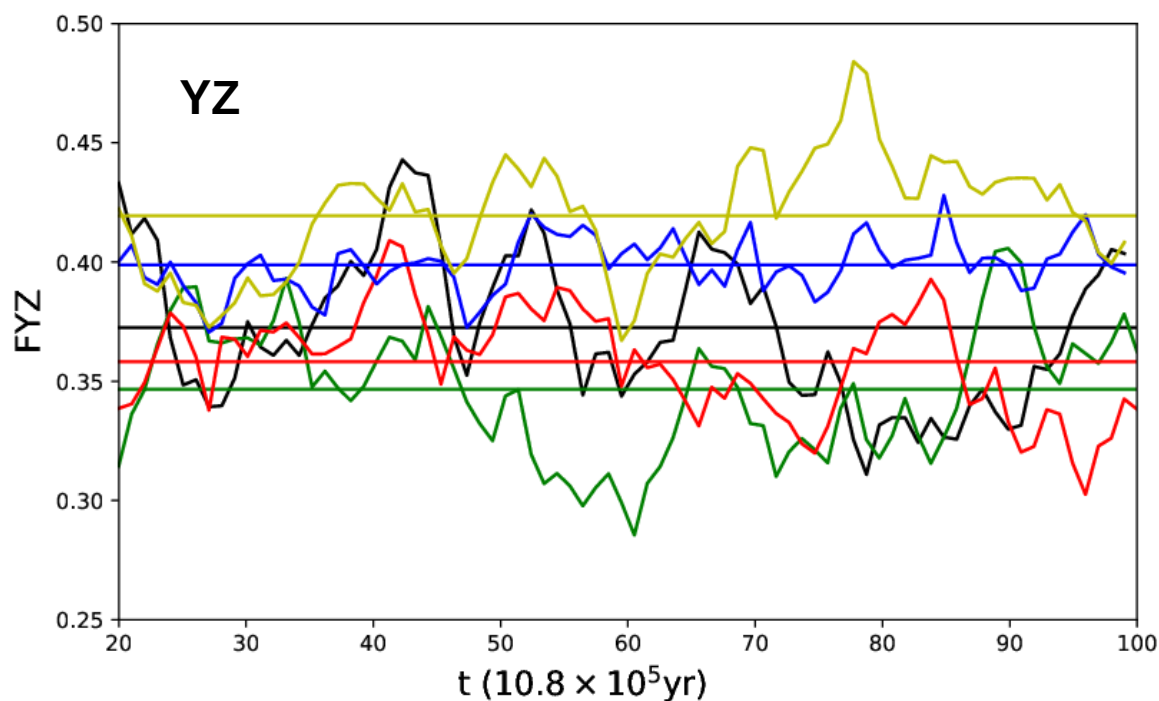
$$\delta_i = \frac{\sum_{j=1}^{512} n_{CNM_j}}{\sum_{j=1}^{512} n_j} \quad \leftarrow \text{CNM mass fraction on the } i\text{-th column}$$

$$f_{2D} = \frac{1}{N+N} \sum_{i=1}^{N+N} \delta_i$$

$$f_{2D0} = \frac{1}{N} \sum_{i=1}^N \delta_i$$

# RESULTS: 2D CNM MASS FRACTION

Villagran & Gazol (submitted)



( $n=2 \text{ cm}^{-3}$ ):  $B_0 = 0.0 \mu\text{G}$ ,  $B_0 \sim 0.4 \mu\text{G}$ ,  $B_0 \sim 2.1 \mu\text{G}$ ,  $B_0 \sim 4.2 \mu\text{G}$ ,  $B_0 \sim 8.3 \mu\text{G}$

**The angle of projection changes the measured CNM mass fraction.**

## RESULTS: MEAN CNM MASS FRACTIONS

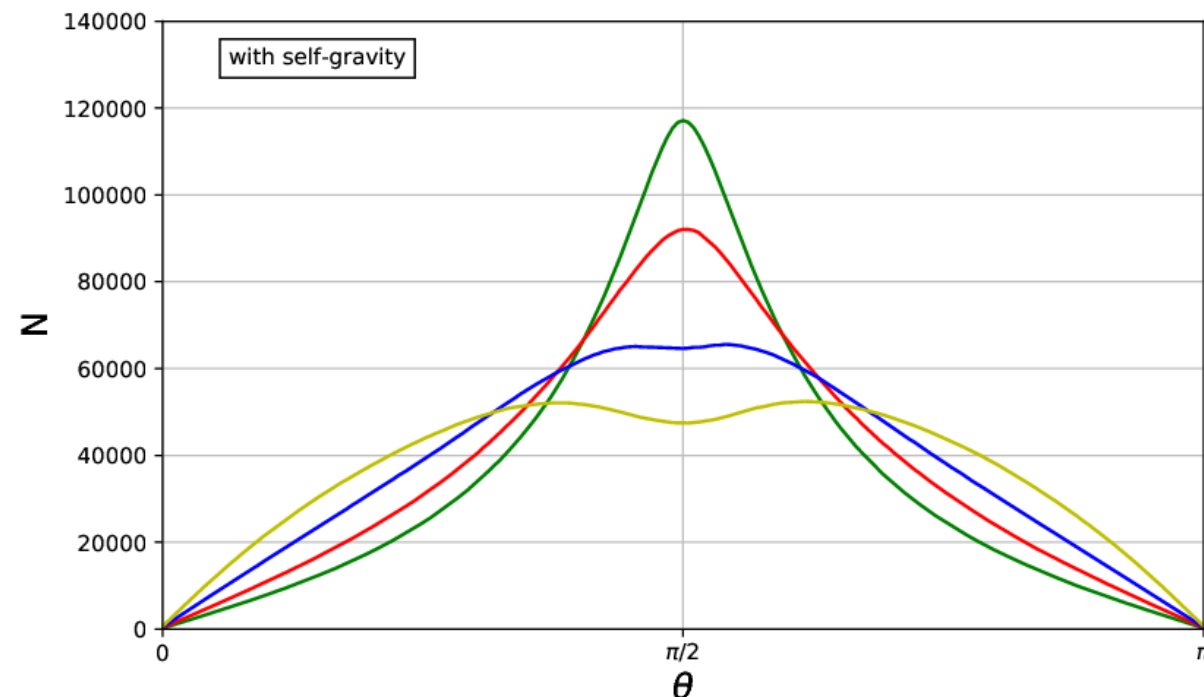
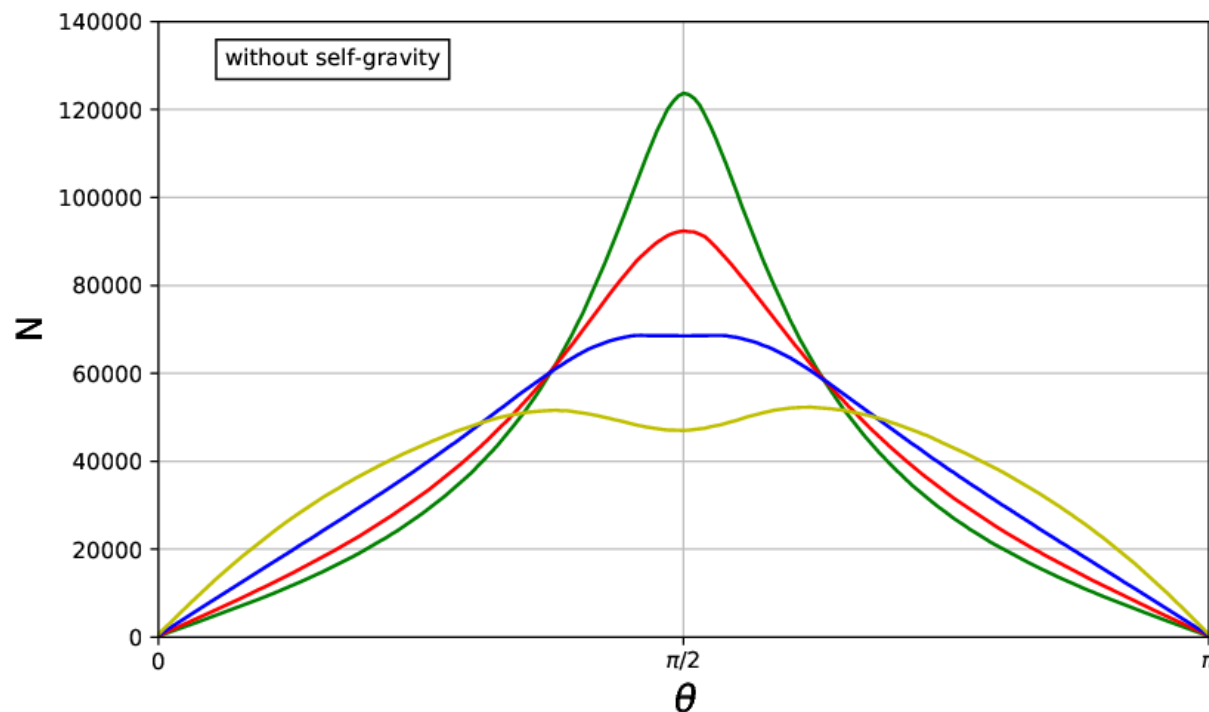
	<b>F3D</b>	<b>FYZ</b>	<b>FXZ</b>	<b>FYZO</b>	<b>FXZO</b>
B00n2	0.59	0.37	0.38	0.46	0.46
B04n2	0.58	0.34	0.35	0.47	0.47
B21n2	0.56	0.36	0.34	0.46	0.46
B42n2	0.52	0.40	0.35	0.45	0.43
B83n2	0.47	0.43	0.33	0.44	0.41
B00Gn2	0.61	0.37	0.38	0.46	0.47
B04Gn2	0.59	0.33	0.34	0.47	0.47
B21Gn2	0.57	0.36	0.35	0.46	0.47
B42Gn2	0.51	0.40	0.36	0.45	0.44
B83Gn2	0.46	0.43	0.33	0.45	0.42

## RESULTS: ALIGNMENT BETWEEN CNM AND $\mathbf{B}$

- Using the technique described in Soler et al. (2013), we estimated the Histograms of Relative Orientation (HRO) for all of our MHD simulations.
- The quantity accounted for in these histograms is the angle between the density gradient and the local  $\mathbf{B}$ .
- We calculated HRO in three-dimensions and in the same two-dimensional projections described before.
- There are virtually no differences between the HRO coming from self-gravitating and non self-gravitating runs.

# RESULTS: 3D HRO FOR THE CNM

Villagran & Gazol (submitted)



( $n=2 \text{ cm}^{-3}$ ):  $B_0 \sim 0.4 \mu\text{G}$ ,  $B_0 \sim 2.1 \mu\text{G}$ ,  $B_0 \sim 4.2 \mu\text{G}$ ,  $B_0 \sim 8.3 \mu\text{G}$

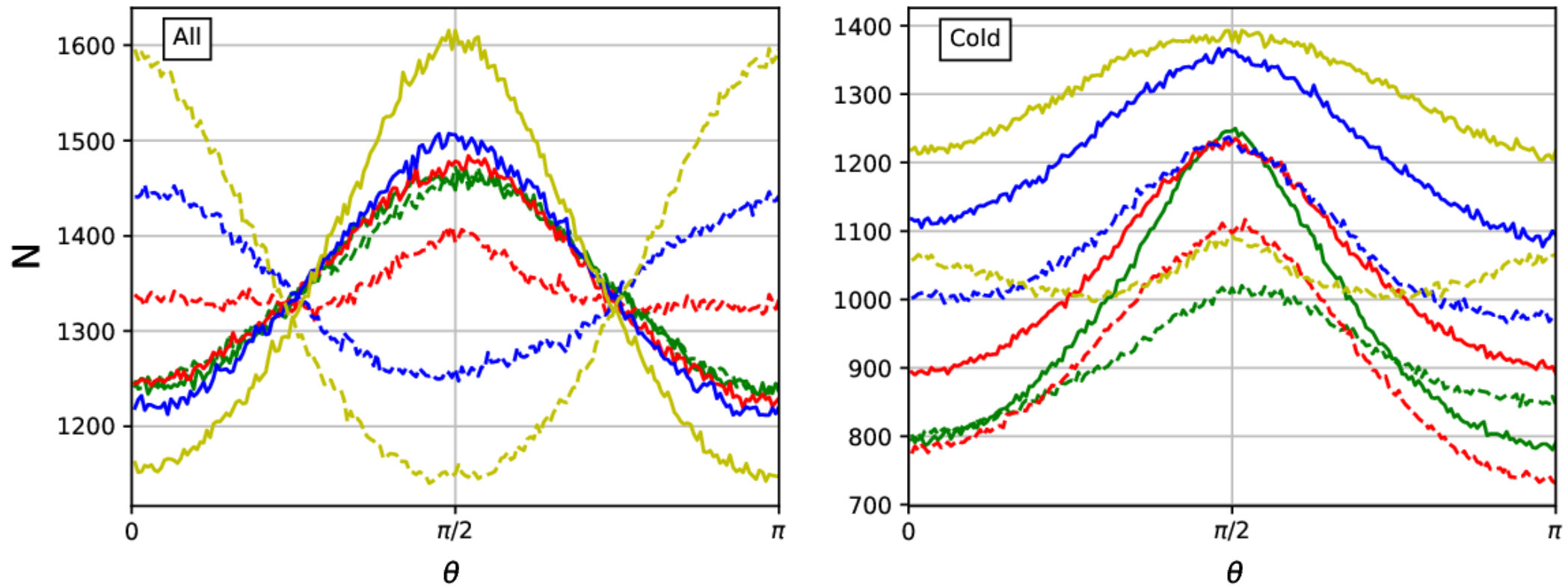
**The intensity of  $B_0$  diminishes the degree of alignment.**

## RESULTS: 2D HRO

- The 2D HRO are calculated for four subsets of the data: **All** (every point in the projection), **Cold** (the projection of the 3D cold cells), **Medium  $\Sigma$**  (the pixels from All with densities between  $10^{20}$  and  $10^{21}$   $\text{cm}^{-2}$ ), and **High  $\Sigma$**  (the pixels from All with densities between  $10^{21}$  and  $10^{22}$   $\text{cm}^{-2}$ ).
- All the histograms were calculated in two projections. The first (continuous line) is perpendicular to the initial magnetic field and the second one (dashed line) is parallel to it.
- The projected magnetic field is a volume weighted quantity along the lines of sight.

# RESULTS: 2D HRO (ALL AND COLD)

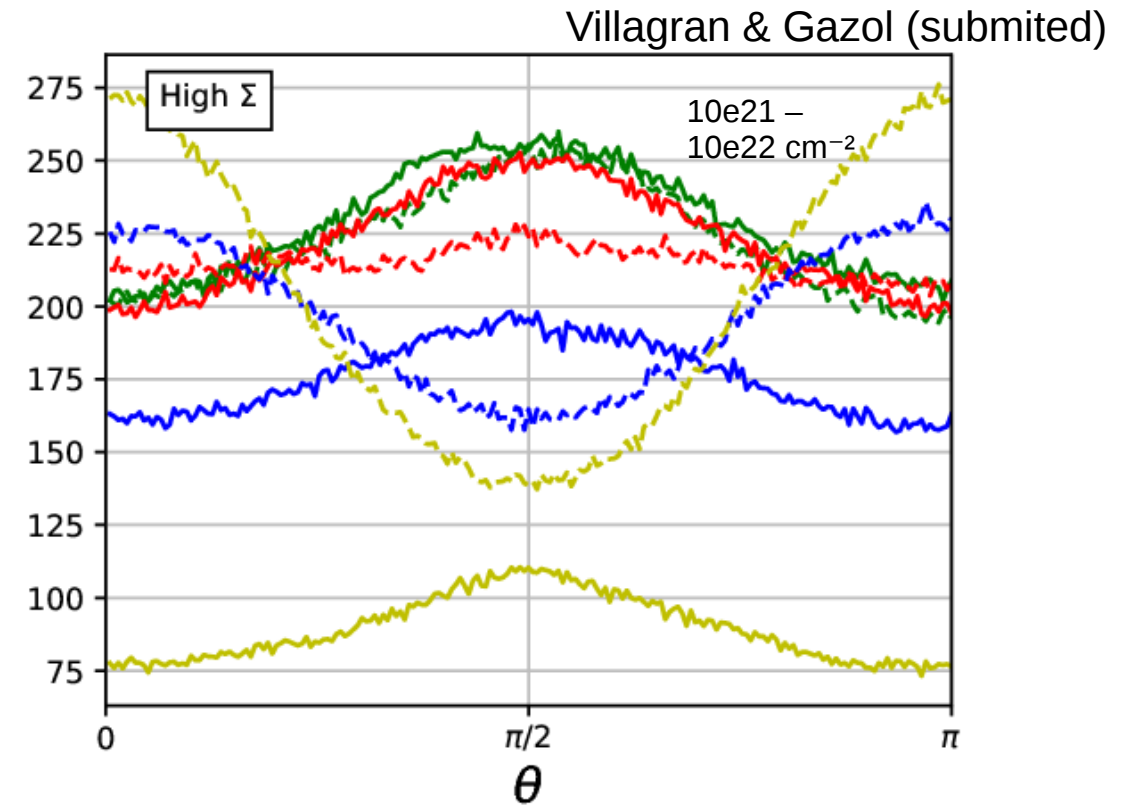
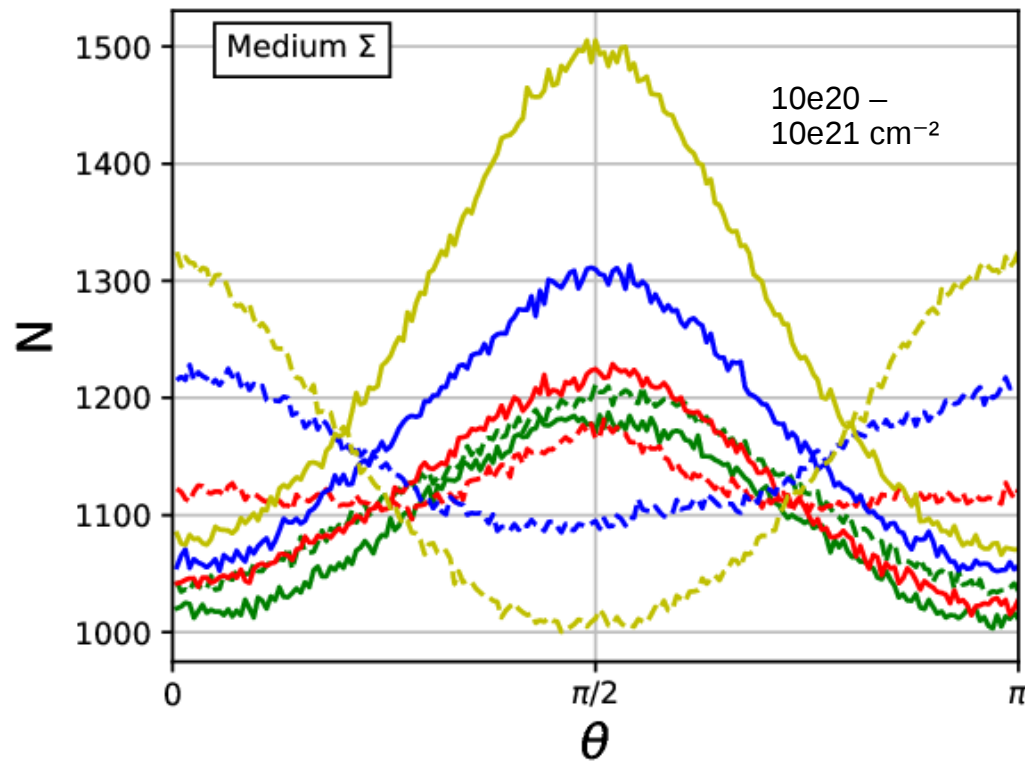
Villagran & Gazol (submitted)



( $n=2 \text{ cm}^{-3}$ ):  $B_0 \sim 0.4 \mu\text{G}$ ,  $B_0 \sim 2.1 \mu\text{G}$ ,  $B_0 \sim 4.2 \mu\text{G}$ ,  $B_0 \sim 8.3 \mu\text{G}$

**The cold gas is aligned independently of projection angle.**

# RESULTS: 2D HRO (MEDIUM $\Sigma$ AND HIGH $\Sigma$ )



( $n=2 \text{ cm}^{-3}$ ):  $B_0 \sim 0.4 \mu\text{G}$ ,  $B_0 \sim 2.1 \mu\text{G}$ ,  $B_0 \sim 4.2 \mu\text{G}$ ,  $B_0 \sim 8.3 \mu\text{G}$

**Column density selections trace All the gas.**

## CONCLUSIONS: CNM MASS FRACTION

- The influence of the magnetic field intensity over the mass fraction of segregated CNM is quite relevant and, for solar neighbourhood conditions, varying its initial value (from  $B_0 = 0.0$  to  $8.3 \mu\text{G}$ ) affects the segregation significantly (variations of 10%).
- In our models the CNM mass fraction is lowered by the presence of  $\mathbf{B}$  and it reaches lower values as the magnetic field intensity increases. This effect appears clearly only when the mass fraction is measured in three dimensions and marginally in two dimensions when only considering lines of sight containing cold gas.
- When the CNM mass fraction is measured only along the lines of sight that have cold gas in them, its average value is mostly independent of projection effects and  $\mathbf{B}$ 's intensity.
- All of our two-dimensional mass fractions are within reasonable agreement with the accepted observational measurements.

## CONCLUSIONS: ALIGNMENT BETWEEN CNM AND $\mathbf{B}$

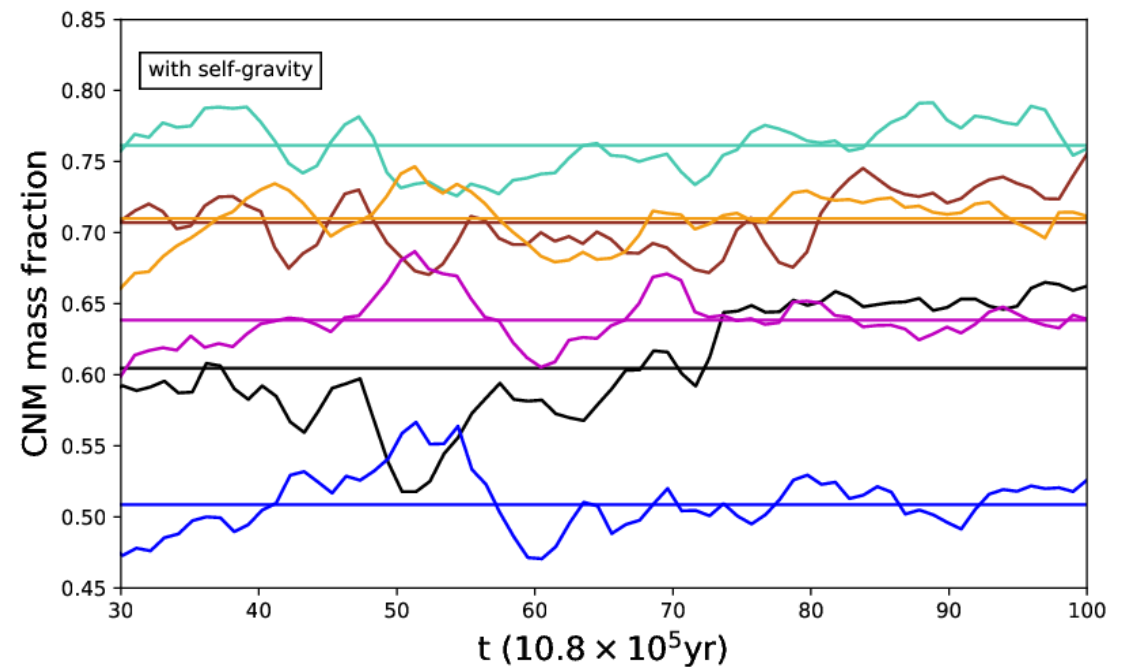
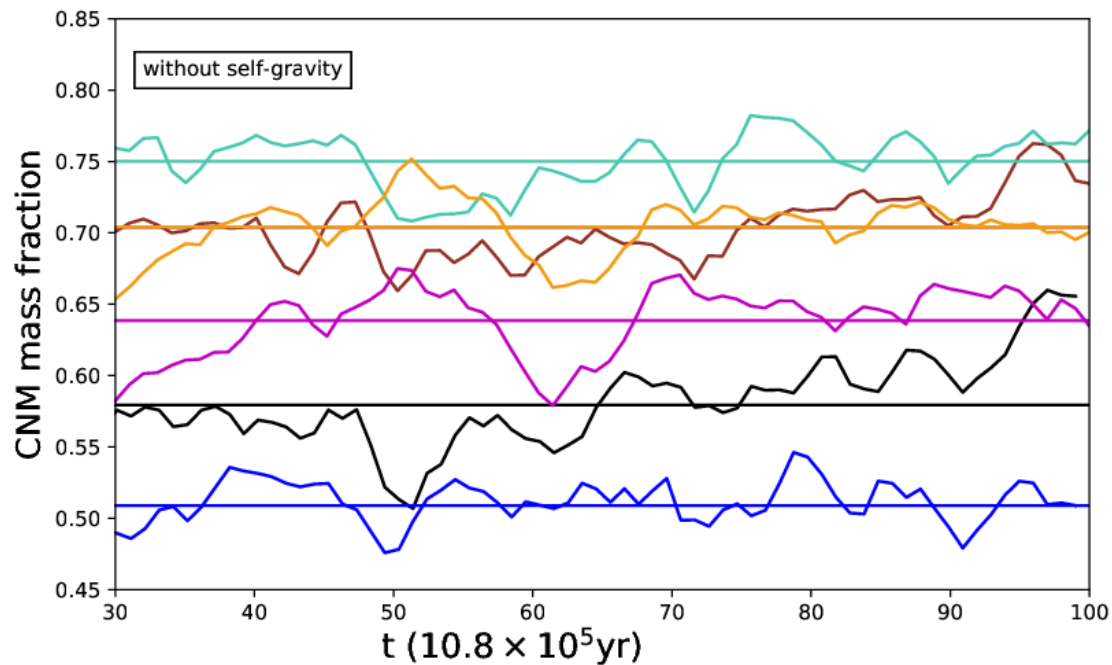
- Cold gas dense structures tend to be aligned with the local magnetic field. This is prevalent in all the studied cases, but the increase in intensity of  $\mathbf{B}$  diminishes the degree of alignment. This tendencies are also observed in two-dimensional projections both in directions parallel and perpendicular to the initial magnetic field.
- The presence of self-gravity does not affect significantly the behaviour of the CNM's mass fraction nor the alignment of cold structures with  $\mathbf{B}$  when using initial mean densities akin to those of the Solar neighbourhood. This could change in a case of decaying turbulence.

---

# FINAL REMARKS

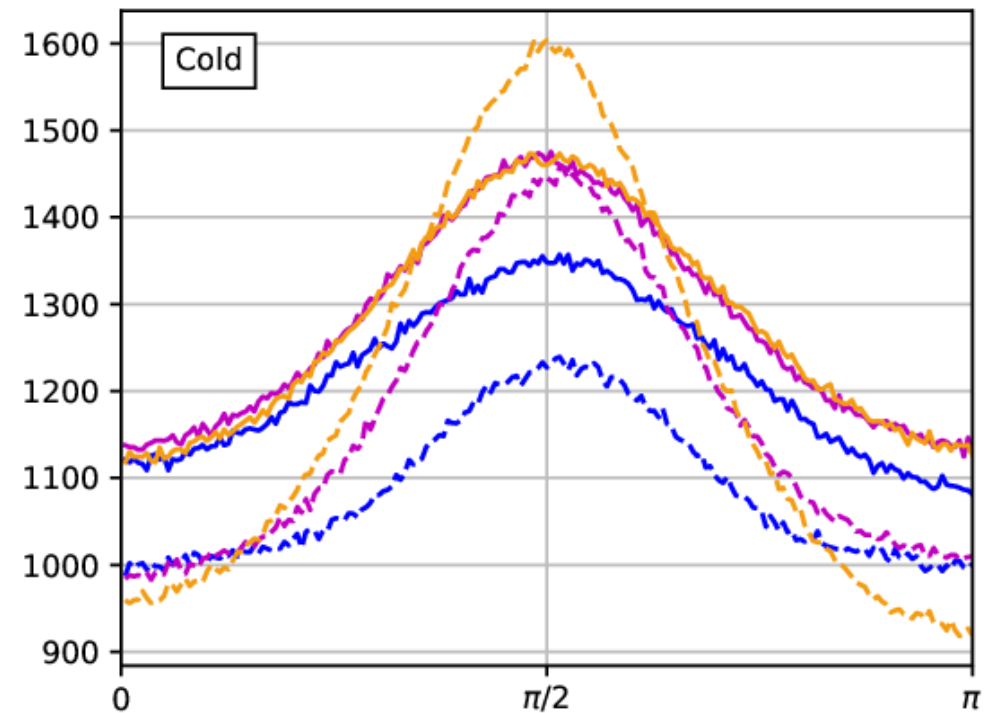
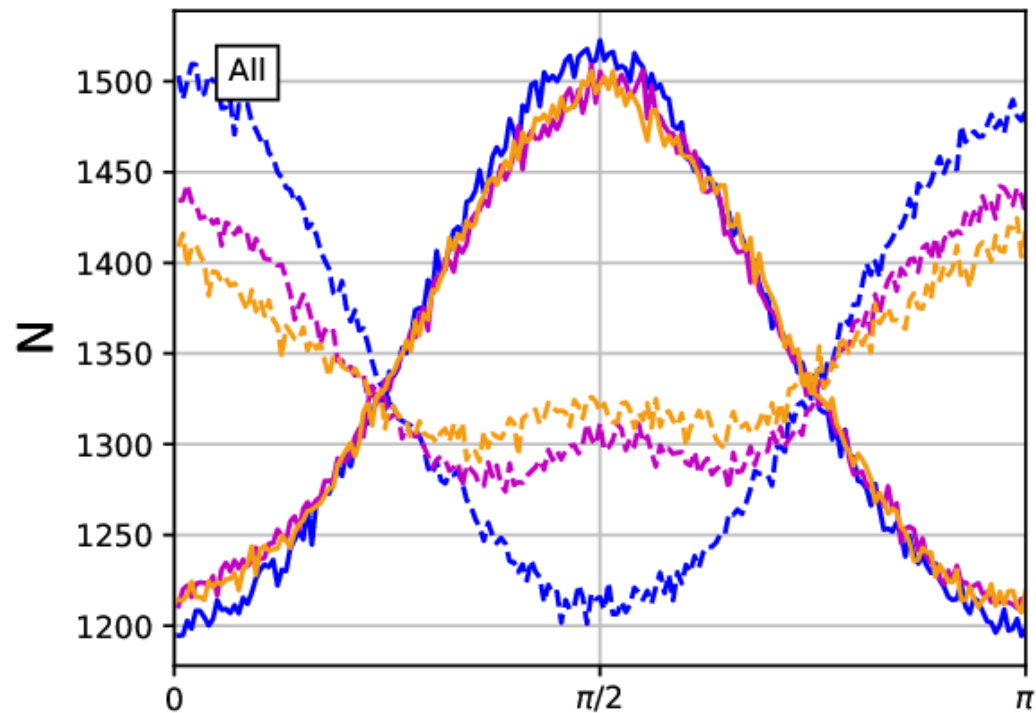
Magnetic field is important in the neutral atomic medium and we should keep studying it with detail.

# BONUS #1: CNM MASS FRACTION HD AND B42



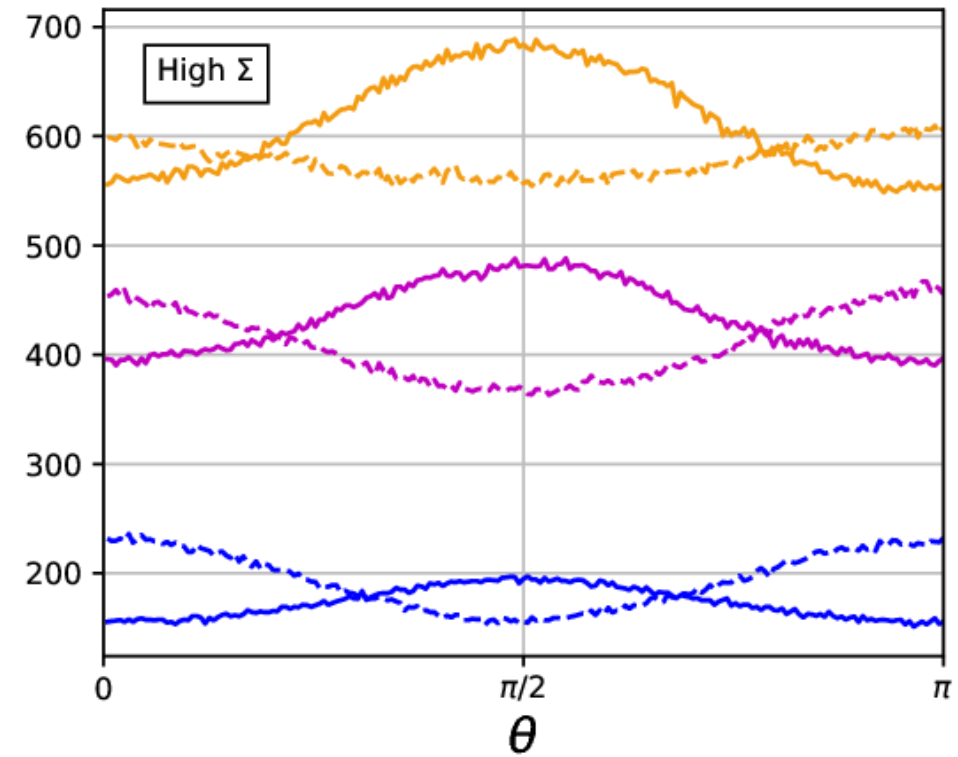
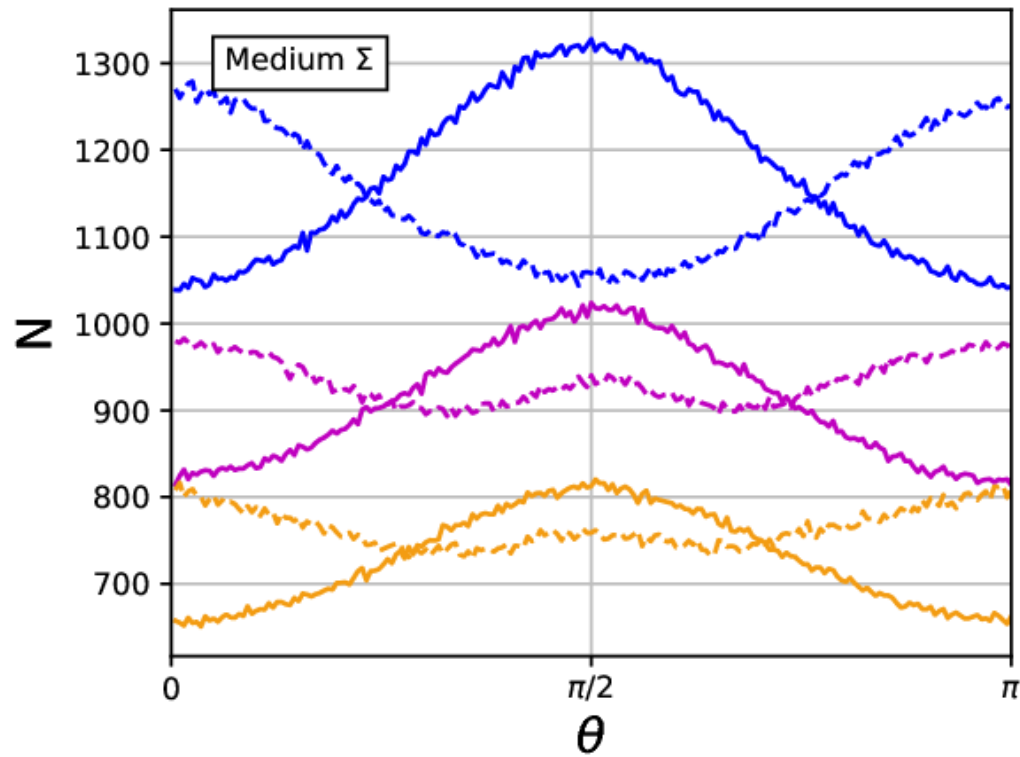
$B_0 = 0.0 \mu\text{G}$  ( $n=2 \text{ cm}^{-3}$ ),  $B_0 \sim 4.2 \mu\text{G}$  ( $n=2 \text{ cm}^{-3}$ ),  $B_0 \sim 4.2 \mu\text{G}$  ( $n=3 \text{ cm}^{-3}$ ),  
 $B_0 = 0.0 \mu\text{G}$  ( $n=3 \text{ cm}^{-3}$ ),  $B_0 \sim 4.2 \mu\text{G}$  ( $n=4 \text{ cm}^{-3}$ ),  $B_0 \sim 0.0 \mu\text{G}$  ( $n=4 \text{ cm}^{-3}$ )

## BONUS #2: HRO FOR B42 (N2, N3 AND N4)



$B_0 \sim 4.2 \mu\text{G}$  ( $n=2\text{cm}^{-3}$ ),  $B_0 \sim 4.2 \mu\text{G}$  ( $n=3\text{cm}^{-3}$ ),  $B_0 \sim 4.2 \mu\text{G}$  ( $n=4\text{cm}^{-3}$ )

## BONUS #2: HRO FOR B42 (N2, N3 AND N4)



$B_0 \sim 4.2 \mu\text{G}$  ( $n=2\text{cm}^{-3}$ ),  $B_0 \sim 4.2 \mu\text{G}$  ( $n=3\text{cm}^{-3}$ ),  $B_0 \sim 4.2 \mu\text{G}$  ( $n=4\text{cm}^{-3}$ )